Conservation of Lateral Momentum in Heterostructure Integrated Thermionic Coolers

Daryoosh Vashaee and Ali Shakouri[*]
Jack Baskin School of Engineering
University of California Santa Cruz, CA 95064

ABSTRACT

Thin film thermionic coolers use selective emission of hot electrons over a heterostructure barrier layer from emitter to collector resulting in evaporative cooling. In this paper a detailed theory of electron transport perpendicular to the multilayer superlattice structures is presented. Using Fermi-Dirac statistics, density-of-states for a finite quantum well and the quantum mechanical reflection coefficient, the current-voltage characteristics and the cooling power density are calculated. The resulting equations are valid in a wide range of temperatures and electric fields. It is shown that conservation of lateral momentum plays an important role in the device characteristics. If the lateral momentum of the hot electrons is conserved in the thermionic emission process, only carriers with sufficiently large kinetic energy *perpendicular* to the barrier can pass over it and cool the emitter junction. However, if there is no conservation of lateral momentum, the number of electrons participating in thermionic emission will dramatically increase. The theoretical calculations are compared with the experimental dark current characteristics of quantum well infrared photodetectors and good agreement over a wide temperature range is obtained. Calculations for InGaAs/InGaAsP superlattice structures show that the effective thermoelectric power factor (electrical conductivity times the square of the effective Seebeck coefficient) can be improved comparing to that of bulk material. We will also discuss methods by which the conservation of lateral momentum in thermionic emission process can be altered such as by creating a controlled roughness at the interface of the superlattice barriers. The improvement in the effective power factor through thermionic emission can be combined with the other methods to reduce the phonon thermal conductivity in superlattices and thus obtain higher thermoelectric figure-of-merit ZT.

I- INTRODUCTION

Heterostructure Integrated Thermionic (HIT) coolers have been recently made and characterized for applications to integrated cooling (See Fig. 1) [1-9]. In these structures a potential barrier is used for the selective emission of hot electrons and evaporative cooling of the electron gas. The HIT cooler could operate in two modes. For a single barrier structure in the strong nonlinear regime, electron transport is dominated by the supply of electrons in the cathode layer [1]. Since only hot electrons (with energy bigger greater than E_f) are emitted above the barrier, electron-electron and electron-phonon interactions try to restore the quasi Fermi distributions in the cathode layer by absorbing

---

[*] ali@soe.ucsc.edu

heat from the lattice, thus cooling the layer. This heat is deposited on the anode side. Theoretical estimates [1,2,16] show that there is an optimal barrier width of the order of a few electron energy relaxation lengths and an optimum barrier height of the order of k_BT, and that such heterostructure coolers can provide 20-30 ^{o}C cooling with KW/cm^2 cooling density. Since the operating currents for the device is very high (10^5 A/cm^2), non-ideal effects such as the Joule heating at the metal-semiconductor contact resistance, and the reverse heat conduction have limited the experimental cooling results to <1 ^{o}C [3]. There is another regime of operation in which electron transport is dominated by the multi barrier structure [10-12]. A superlattice is chosen so that hot electrons move easily in the materials, but the movement of cold electrons is more restricted. In this case, there will be also net cooling in the cathode layer and heating in the anode layer. Estimates show that small barrier height on the order of k_BT does not give much improvement over bulk thermoelectric materials [13-15], and it was suggested to use tall barriers and high doping densities to achieve a large number of electrons moving in the material [4]. In this paper the latter regime of transport is investigated in detail and it is shown that conservation of the lateral momentum plays an important role in the device performance. There have been several recent theoretical studies of electron transport in single barrier and superlattice structures where thermionic emission and conventional thermoelectric cooling are compared [13-15]. These studies mainly focus on the ballistic transport in thin barriers and did not consider the effect of lateral momentum conservation.

Figure-1a shows a single-element superlattice micro cooler.
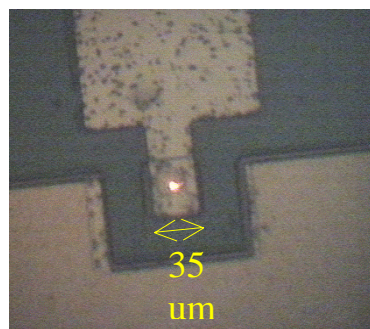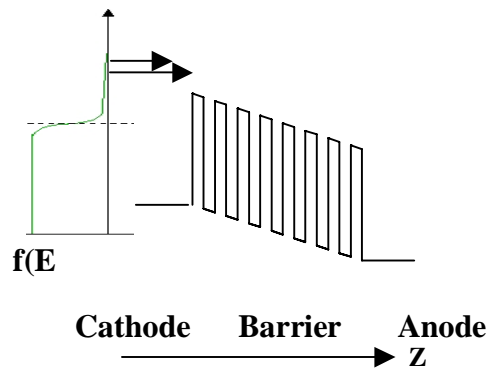
(a)   **(b)**

Figure-1: (a) Top view of a heterostructure integrated thermionic (HIT) micro-cooler taken by an optical microscope. (b) Schematic energy diagram along with electron energy distribution and energy fermi level

Figure 1-b shows the energy diagram of a typical superlattice micro cooler. Cooling is proportional to the number of electrons involved in thermionic emission. Only electrons that have kinetic energy in z-direction higher than the barrier height can pass over the barrier and participate in thermionic cooling. Number of those electrons can be calculated for a given temperature according to:

$$n_e(V) = \sum_{E_i} \int_{E_i}^{\infty} D(E)f(E,E_f)[1 - f(E, E_f - qV)]T(E)dE \qquad (1)$$

Where $D(E)$ is electron density of states, f is the Fermi-dirac distribution, and $T(E)$ is the transmission probability for the electrons to pass the barrier. E_i is the quantized energy level in the well. Similar expression is often used for the calculation of dark current in quantum well infrared photodetectors (QWIPs) [2,3], but they ignored the *(1-f)* term, which is negligible when the Fermi level is deep in the well. In the case of HIT coolers the Fermi level should be close to the barrier height to achieve large cooling powers. For the latter case, one should check for the availability of empty states at the neighboring well and the *(1-f)* term should be included. While equation 1 predicts very well the dark current in quantum well photodetectors (see appendix and Ref. [2]), one should consider several other important factors for the calculation of thermionic current and cooling power density for HIT coolers. Section II and III describe the details of the calculations depending on the conservation of lateral momentum.

II- NON-CONSERVATION OF LATERAL MOMENTUM

Equation 1 implies the fact that the transmission probability, $T(E)$, depends on the total energy of the electron. This is valid only when there is scattering. Without any scattering electron motion in z-direction and in x-y plane is decoupled and one should change $T(E)$ to $T(E_0)$ in equation (1), which means that the transmission probability depends on the quantized energy inside the well. This will significantly decrease the number of electrons passing the barrier. The role of scattering has been studied in detail by Meshkov [21] for the case of carrier tunneling in the barrier. In the absence of electron-electron interaction and inhomogeneities, the motion in the xy plane is completely separable from the quantized longitudinal motion, and electron wave function decays into barrier with the characteristic exponential

$$\psi \ \alpha \ \exp\left(-\int dz\{2m[V(z) - E_i]\}^{1/2}/\hbar\right) \qquad (2)$$

Where $V(z)$ is the potential in the barrier, and E_i is the quantized electron energy in the well.

This means that the tunneling exponent is independent of the kinetic energy $K = p^2/2m$ of the electron motion in xy plane. The situation will be different in the presence of scattering, which mixes different degrees of freedom. It has been shown by Meshkov that however weak the scattering processes, the asymptotic decay law for the electron density is described by a wave function that result if the carriers had tunneled in the one-dimensional potential V(z) but with the total Energy $E = E_0 + K$ [21] :

$$\psi \ \alpha \ \exp\left(-\int dz\{2m[V(z) - E]\}^{1/2}/\hbar\right) \qquad (3)$$

It is important to notice that the decay rate of equation 3 is valid only at sufficiently large distances from the QW. Transition to the no-scattering limit is described by a pre-exponential factor, which depends on the specific scattering mechanism. The weakness of

the scattering mechanisms leads to a small pre-exponential correction factor for the unperturbed wave function and essentially affects the distance from the QW at which equation (3) can be used [24]. Experimental observations in the strong scattering regime have confirmed the non-conservation of lateral momentum in the exponential decay of wavefunction [25]. In the case of weak scattering the regime of validity for Meshkov's argument is much further away from the QW and thus it does not affect measurable physical quantities [24]. This situation is shown in figure 2.
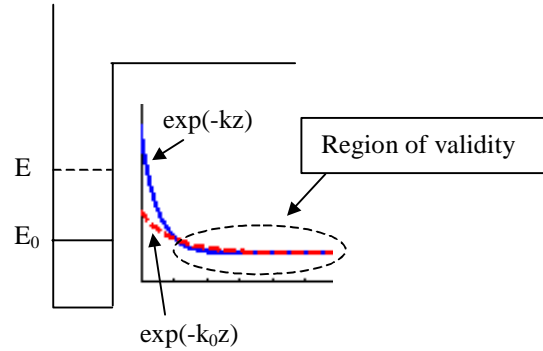
Figure 2: Penetration of a quantum-well wave function into the confining barrier. In the absence of scattering, all the states belonging to the same subband E_0 decay asymptotically as proportional to exp(-k_0z). In the presence of scattering, however weak, the asymptotic decay is proportional to exp(-kz) and depends on the in-plane kinetic energy. That is valid at a large distance from the well.

We hereby study the two limiting cases of no-scattering and strong momentum scattering for the calculation of the thermionic current and the heat flux, and compare the effective dimensionless figure of merit **ZT** in these two limits.

II- CONSERVED LATERAL MOMENTUM CASE

We will first calculate the thermionic current for the case of no-scattering. In this case, the longitudinal (z) component of the wave function can be separated from the other degrees of freedom and the lateral momentum is conserved. One can use equation 1 with a two dimensional density of states when the Fermi level is deep inside the well, similar to the case of quantum well photodetectors. However, the Fermi level in heterostructure thermionic coolers is close to the top of the barrier and one needs to consider the contribution of the electronic states above the barrier in the calculation of thermionic current. Figure 3 shows a schematic energy diagram for two neighboring well. E_1 and E_2 are two quantized energy levels, E_f is the Fermi level, and E_b is the barrier height. Figure 5-b shows k_1, k_2, k_f, and k_b , which are the wave-vectors corresponding to the latter energies $E = \dfrac{\hbar^2 k^2}{2m}$.
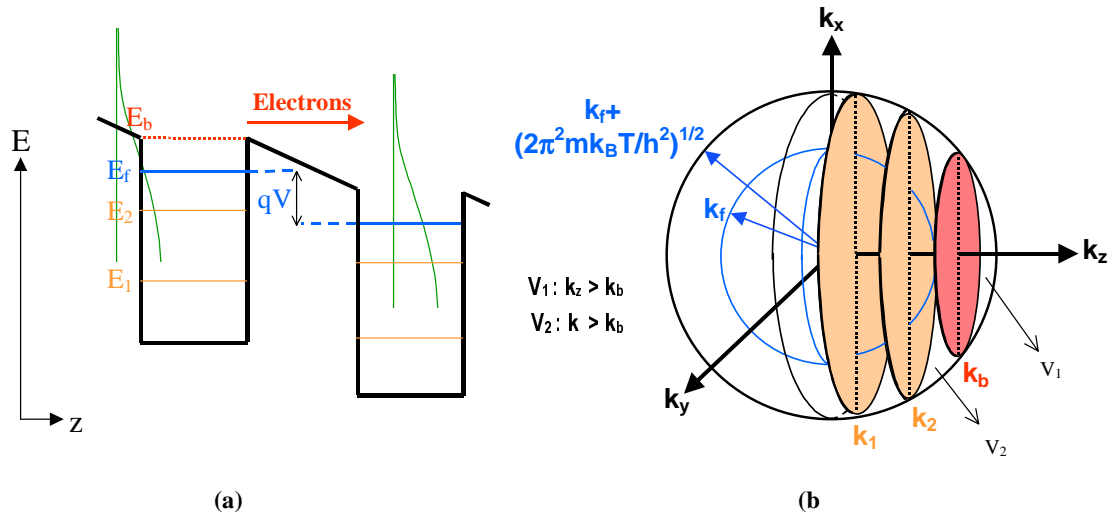
Figure 3: (a) Conduction band and energy levels of two neighboring wells (b) Corresponding wave-vectors in the k-space: k_1, k_2, and k_b correspond to cross sectional planes and k_f is the radius of the Fermi sphere. V_1 is the volume of the electrons that participate in thermionic emission above the barrier if the lateral momentum is conserved. V_2 is that volume if the lateral momentum is not conserved.

Since states with $k_z > k_b$ are not confined in the QW, one can not use a two dimensional density of states. Number of electrons that participate in thermionic emission process can be written directly as an integral in $k_x k_y k_z$ space:

$$n_e(V) = \tag{4}$$

$$\frac{2}{4\pi^2} \sum_i \int_0^\infty dk_x \int_0^\infty dk_y f(k_x, k_y, k_{z_i}, E_f)[1 - f(k_x, k_y, k_{z_i}, E_f - qV)]T(k_{z_i}, V)$$

$$+ \frac{2}{8\pi^3} \int_0^\infty dk_x \int_0^\infty dk_y \int_{k_b}^\infty dk_z f(k_x, k_y, k_z, E_f)[1 - f(k_x, k_y, k_z, E_f - qV)]T(k_x, k_y, k_z, V)$$

V is the applied voltage. First integral gives the contribution to the transmitted electrons from the quantized energy levels of the well, corresponding to planes k_1, and k_2 in figure 5-b. Transmission probability T depends only on V, and k_{z_i} value since we have assumed that the lateral momentum is conserved. Second integral is the number of transmitted electrons from the energy band above the barrier, corresponding to the states in volume V_1 in figure 5-b. Equation 4 can be simplified by letting $k = \sqrt{k_x^2 + k_y^2}$:

$$n_e(V) = \sum_i \int_0^\infty dk \frac{k}{\pi} f(k,k_{z_i},E_f)[1 - f(k,k_{z_i},E_f - qV)]T(k_{z_i},V) \qquad (5)$$

$$+ \int_0^\infty dk \int_{k_b}^\infty dk_z \frac{k}{2\pi^2} f(k,k_z,E_f)[1 - f(k,k_z,E_f - qV)]T(k,k_z,V)$$

To calculate thermionic figure-of-merit, one needs to obtain the energy transported by these electrons. We will use the following quantity in calculation of thermionic power Q.
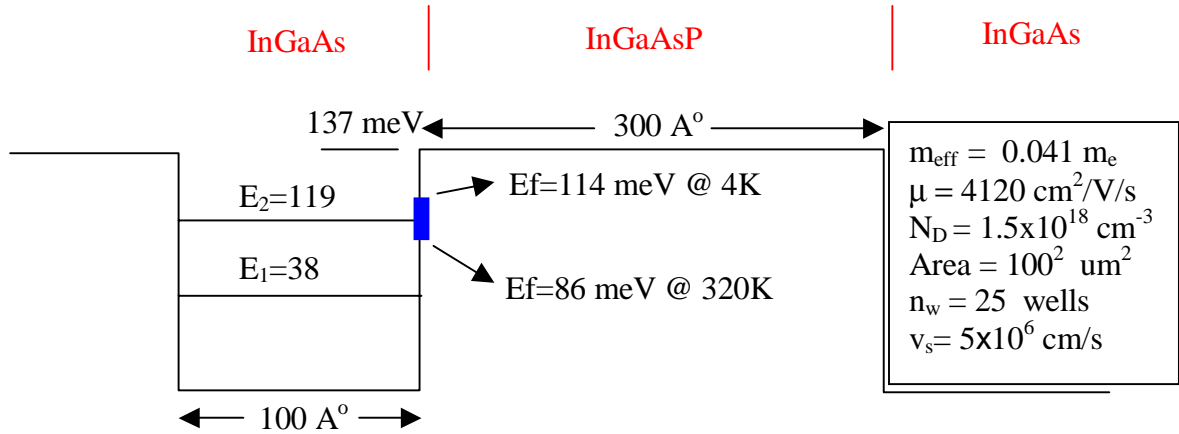
$$n_Q(V) = \qquad (6)$$

$$\frac{\hbar^2}{2\pi\,m} \sum_i \int_0^\infty dk k(k^2 + k_{z_i}^2 - k_f^2) f(k,k_{z_i},E_f)[1 - f(k,k_{z_i},E_f - qV)]T(k_{z_i},V)$$

$$+ \frac{\hbar^2}{4\pi^2 m} \int_0^\infty dk \int_{k_b}^\infty dk_z k(k^2 + k_z^2 - k_f^2) f(k,k_z,E_f)[1 - f(k,k_z,E_f - qV)]T(k,k_z,V)$$

This equation is similar to equation 6 except that the integrand is multiplied by difference of the energy of emitted electrons from the Fermi level.

III- NON-CONSERVED LATERAL MOMENTUM

Interaction of the quantized charge carriers in the quantum well, both with each other and with inhomogeneities, couples the in-plane and perpendicular to the plane degrees of freedom. Thus, the lateral momentum is not conserved during thermionic emission, and in this case the transmission probability depends on the total energy of electron, and not just the kinetic energy perpendicular to the well [21,22]. One thus replaces $T(k_z,V)$ with $T(k,k_z,V)$ in the first term of equations 4,5 and 6.

Let's now consider a specific HIT cooler structure in the two limiting regimes conserved and no-conserved lateral momentum. The structure consists of 25 periods of InGaAs/InGaAsP superlattice lattice matched to InP substrate. Widths of the well and barrier are 10 nm and 30 nm, respectively, the wells are doped to 1.5×10^{18} cm^{-3}, and the device size is taken to be 10^4 μm^2. Figure 4 shows the band diagram. Barrier height is about 137 meV. E_1 and E_2 are the quantized energy levels inside the well.

InGaAs   InGaAsP   InGaAs

137 meV ← 300 A° →

$E_2 = 119$

$\rightarrow$ Ef=114 meV @ 4K

$E_1 = 38$

$\searrow$ Ef=86 meV @ 320K

$m_{eff} = 0.041\ m_e$
$\mu = 4120\ cm^2/V/s$
$N_D = 1.5 \times 10^{18}\ cm^{-3}$
$Area = 100^2\ um^2$
$n_w = 25\ wells$
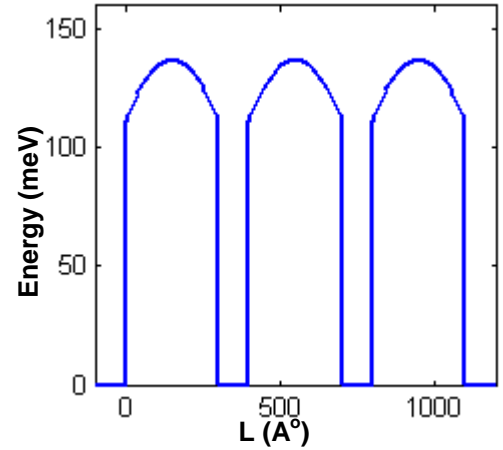$v_s = 5 \times 10^6\ cm/s$

← 100 A° →

Figure 4: InGaAs/InGaAsP superlattice structure.

Since only the wells regions are doped, the band diagram in figure 4 is not square barrier. Figure 5 shows the self consistant calculation of the conduction band profile, using poisson equation. Since the Fermi level is close to top of the barrier, one should consider the 3D states above the barrier, and also the variation of Fermi level with temperature should be included. Fermi level increases from 84 meV at 320K to 113 meV at 4K.

Fermi level can be calculated from the following relation for carrier concentration:

Figure 5: Self consistent energy band calculation for the superlattice structure of figure 4.

$$N_D = \frac{1}{L_W} \sum_i \int_0^\infty dk \frac{k}{\pi} f(k, k_{z_i}, E_f) + \frac{L_W + L_b}{L_W} \int_0^\infty dk \int_{k_b}^\infty dk_z \frac{k}{2\pi^2} f(k, k_z, E_f)$$

Figure 6: Fermi energy for the structure of figure 4 with E_b of 133 meV. Dotted curve correspondes to the values if only 2D states of the well are considered in the calculations. Solid line is for when the 3D states above the barriers are taken into account too.

Only 2D DOS

14 meV

2D + 3D DOS
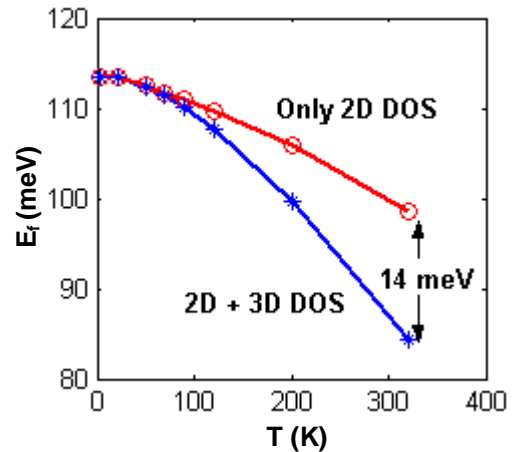
N_D is the doping (in cm^{-3}) in the well region. First integral gives the number of electrons confined in the well and the second integral is the electrons in 3D states above the barrier. The $1/L_W$ factor in the first term is to transform the 2D density of states to the 3D doping in the well. Since only the well regions are doped, the $(L_W+L_b)/L_W$ factor in front of the second integral is to consider the non-uniform doping.

Figure 6 shows the Fermi level vs. temperature for the structure of figure 4. For a comparison we have plotted the Fermi level if we ignore the 3D states above the barrier. It shows that at low temperatures electrons are mostly confined inside the well and one can ignore barrier states, but at higher temperature the contribution from barrier states should be taken into account for the calculation of thermionic current.

Figure 7 shows the transmission probability calculated using WKB approximation for the structure of figure 4. For comparison we have plotted the transmission probability with the square barrier potential profile as well. Since the barrier height changes with applied voltage for the case of parabolic barrier, the transmission probability increases at lower energies for higher applied voltages.
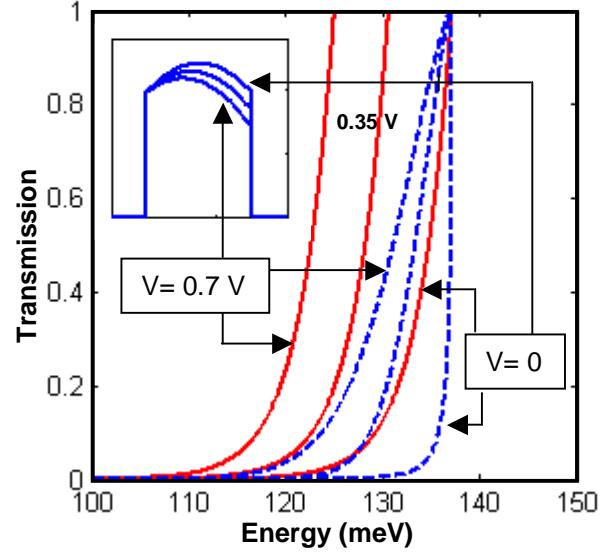
Figure 7: Transmission probability for the structure of figure 4 assuming square well-barrier (dashed curves) and the self consistent potential from figure 5. Inset shows the energy diagram.

IV- HIT Cooler Performance assuming Conserved Lateral Momentum

We thus calculate thermionic current from $I=qn_e(V)vA$. A is the area of micro cooler, and v is electron drift velocity given by:

$$v = \frac{\mu F}{\sqrt{1+\left(\dfrac{\mu F}{v_s}\right)^2}} \qquad (8)$$

Where μ is the mobility, v_s is the saturation velocity, and F is the electric field in the barrier. Similarly, thermionic cooling power can be calculated from:

$$Q = n_q vA \qquad (9)$$

In analogy with thermoelectrics, one can define thermionic figure-of-merit as:

$$ZT = \frac{\sigma S^2}{\beta}T \qquad (10)$$

where β is the thermal conductivity of the material and S is the effective seebeck coefficient that can be calculated from Q and I according to:

$$S = \frac{Q}{IT} \qquad (11)$$

and σ is the effective conductivity that can be calculated from I, V according to:

$$\sigma = \frac{IL_p n_w}{AV} \qquad (12)$$

where L_p is the period of the superlattice, and n_w is the number of wells. One should note that since in general we are in non-linear transport regime, the effective seebeck and conductivity are
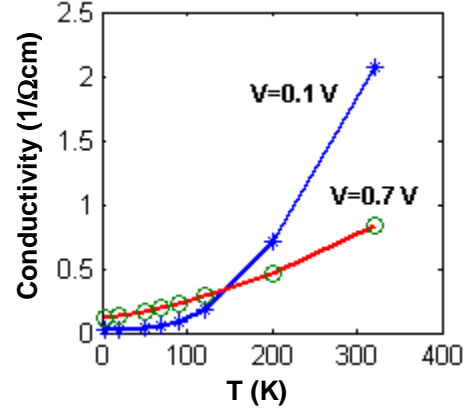
Figure 8: Effective conduc-tivity vs. temperature for the structure of figure 6 assum-ing conserved lateral mom-entum.
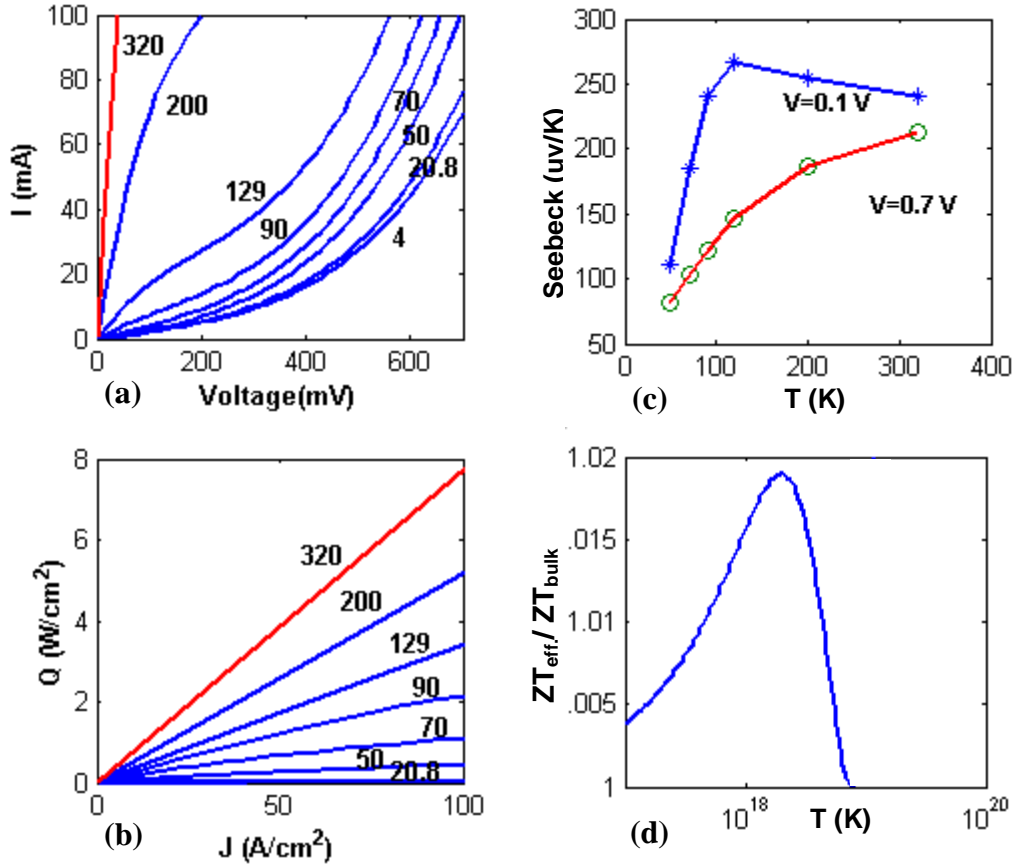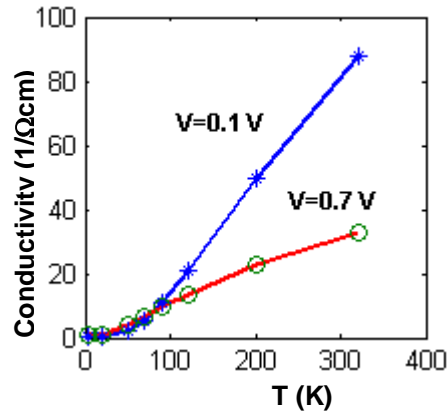
Figure 9: (a) Current vs. voltage, (b) thermionic cooling power, (c) equivalent seebeck coefficient, and (d) ratio of effective thermionic figure-of-merit to that of bulk InGaAs for the structure of figure 4 assuming conserved lateral momentum. Thermal conductivity of the superlattice is assumed to be the same as bulk InGaAs (5 W/mK).

voltage dependent. However at room temperature the I-V curve is approximately linear at low voltages and the effective σ and S can be used for comparison with thermoelectric coolers. Figure 8 shows the calculated conductivity for structure of figure 5 assuming conserved lateral momentum. Figures 9-a and 9-b show the current versus voltage and cooling power densities versus current for different temperatures in the case of conserved lateral momentum. Figures 9-c, and 9-d show the corresponding effective seebeck coefficient, and ratio of effective thermionic figure-of-merit to that of bulk InGaAs. The contribution of thermionic cooling increases the bulk thermoelectric effect by a very small amount (~1.7%).

V- HIT Cooler Performance assuming Non-conserved Lateral Momentum

Figure 10 shows the conductivity of the same structure with the assumption that lateral momentum is not conserved. It can be seen that that the conductivity is about 40 time larger than that of conserved lateral momentum. This large increase in conductivity is expected by looking at figure 3-b and number of states available in volume V_1 compared to those available in volume V_2. Figures 11-a to 11-e show the similar curves as 10-a to 10-e but assuming that the lateral momentum is not conserved.

It can be seen that thermionic current is significantly increased. The contribution of thermionic cooling has increased by a factor of 40 compared to that of conserved lateral momentum case (~70%). Thus the overall thermionic figure-of-merit has improved by factor of 1.7 compared to the bulk **ZT** of InGaAs (or InGaAsP).

Figure 10: Effective conduc-tivity vs. temperature for the structure of figure 5 assum-ing non-conserved lateral momentum.
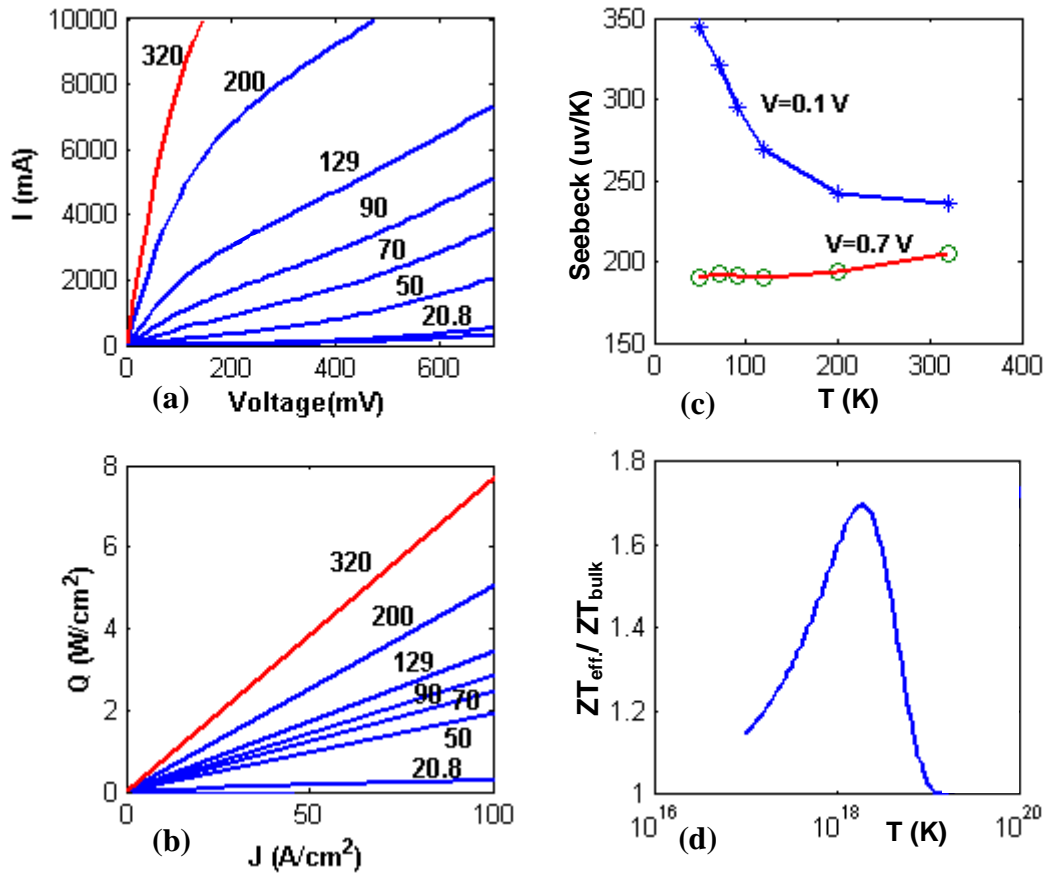
Figure 11: (a) Current vs. voltage, (b) thermionic cooling power, (c) equivalent seebeck coefficient, and (d) ratio of effective thermionic figure-of-merit to that of bulk InGaAs for the structure of figure 4 assuming non-conserved lateral momentum. Thermal conductivity of the superlattice is assumed to be the same as bulk InGaAs (5 W/mK). Thermal conductivity of the superlattice is assumed to be the same as bulk InGaAs (5 W/mK).

CONCLUSION

We described detailed calculation of thermionic current in Heterostructure Integrated Thermionic (HIT) micro coolers. We studied two limiting cases to determine the number of electrons participating in thermionic emission process, based on the conservation of lateral momentum. Strong scattering can mix the planar motion of carriers with longitudinal one (perpendicular to the barrier) and remove the requirement for the conservation of lateral momentum. Therefore, in the latter case, transmission probability depends on total kinetic energy of the electrons, and not only the perpendicular component to the barrier. This will dramatically increase the number of electrons that are transmitted over the barrier. These electrons are responsible for thermionic cooling, and thereby thermionic figure of merit is increased. Conservation of lateral momentum is a consequence of translational invariance in the plane of QW. It is possible by introducing controlled roughness at interface to break this translational invariance and increase the thermionic cooling power density. It is important to note that the roughness can also

decrease the electron mobility in the material and increase joule heating. However experimental results with GaAs/AlGaAs QWIPs show that it is possible have lateral momentum non-conserved without affecting much the mobility of carriers moving above the barrier (see appendix). Controlled roughness of the superlattice interfaces during the growth or taking advantage of well designed quantum dot structures can create the required inhomogeneities [17]. The improvement in the effective power factor through thermionic emission can be combined with the other methods to reduce the phonon thermal conductivity in superlattices and thus obtain higher thermoelectric figure-of-merit ZT [18-20].

APPENDIX: Dark Current in QWIPs:

Figure 12 shows dark current measured and calculated for a GaAs quantum well infrared photodetectors (QWIP) from reference [22]: The structure consists of 50-period multiquantum well superlattice with 4 nm GaAs well and 30.5 nm $Al_{0.29}Ga_{0.71}As$ barriers. The quantum well region were doped to $N_D = 1.4 \times 10^{18}$ cm^{-3}. The figure shows a good agreement between theory and experiment as a function of both bias voltage and temperature over a range of eight orders of magnitude in dark current. For comparison these curves are re-plotted in figure 13-a from equations 1 and 8 in this paper, which shows the consistency of the calculations.
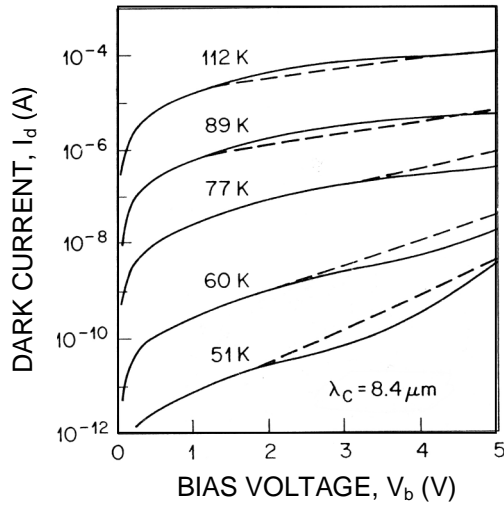
Figure 12: (a) Experimental (solid curves) and theoretical (dashed) dark current-voltage characteristics curves at various temperatures from reference [22]

Figure 13-b shows the same curves for dark current but assuming that the lateral momentum is conserved. At higher temperatures electron energy distribution is extended to higher energies which causes higher dark current in figure 13-a. However, when the lateral momentum is conserved, dark current does not change with temperature. That is because transmission probability no longer depends on the total energy of electrons but on quantized energies in the well which do not change with temperature, and because the contribution of electrons in three dimensional states above the barrier is ignored, as of reference [22], knowing that the Fermi level is located deep in the well.
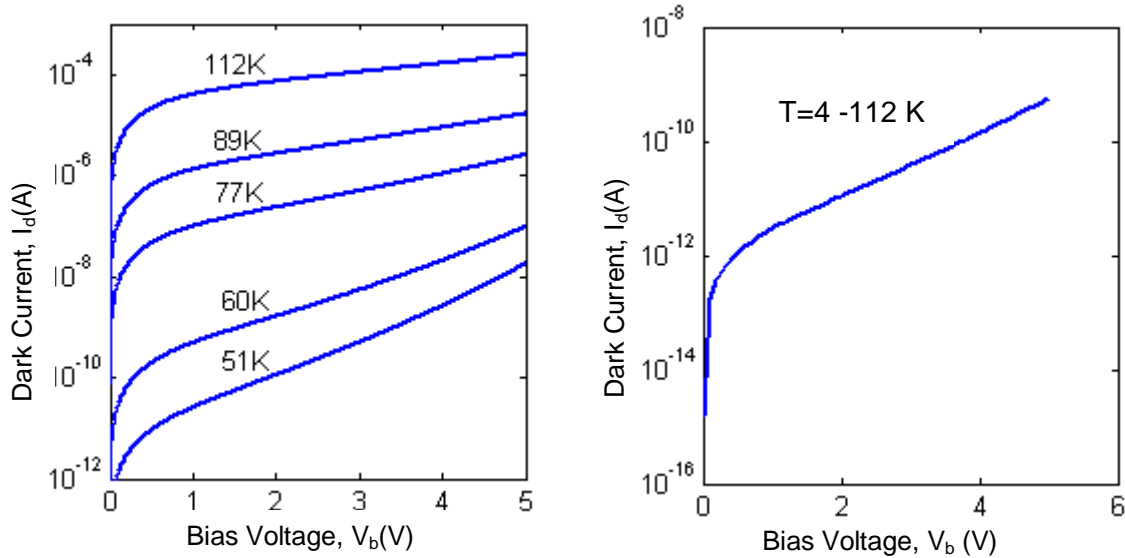
Figure 13: (a) Theoretical curves for the same structure as figure 12 calculated from from equation 1. (b) Similar curves with the assumption of conserved lateral momentum.

ACKNOWLEDGEMENT

REFRENCES

[1] Shakouri, A. and J.E. Bowers, 1997, "Heterostructure Integrated Thermionic Coolers," Applied Physics Letters, **71**, pp. 1234-1236.

[2] Shakouri, A., Lee, E.Y., Smith, D.L., Narayanamurti, V., and Bowers, J.,E., 1998, "Thermoelectric Effects in Submicron Heterostructure Barriers," Microscale Thermophysical Eng., **2**, pp. 37-42.

[3] Shakouri, A., LaBounty, C., Piprek, J., Abraham, P., and Bowers, J.E., 1999, "Thermionic Emission Cooling in Single Barrier Heterostructures," Applied Physics Letters, **74**, pp. 88-89.

[4] Shakouri, A., Labounty, C., Abraham, P., Piprek, J., and Bowers, J.E., 1998, "Enhanced Thermionic Emission Cooling in High Barrier Superlattice Heterostructures", *Material Research Society Symposium Proceedings*, Vol. 545, pp.449-458.

[5] Zeng, G.H., Shakouri, A., La Bounty, C., Robinson, G., Croke, E., Abraham, P., Fan, X.F., Reese, H., and Bowers, J.E., 1999, "SiGe Micro-Cooler," Electronics Letters, **35**, 2146-2147.

[6] Fan, X.F., Zeng, G.H., LaBounty, C., Bowers, J.E., Croke, E., Ahn, C.C., Huxtable, S., Majumdar, A., and Shakouri, A., 2001, "SiGeC/Si Superlattice Microcoolers," Applied Physics Letters, **78**, 1580-1582.

[7] Fan, X.F., Zeng, G., Croke, E., LaBounty, C., Ahn, C.C., Vashaee, D., Shakouri, A., and Bowers, J.,E., 2001, "High Cooling Power Density SiGe/Si Micro-coolers," Electronics Letters, **37**, pp. 126-127.

[8] LaBounty, C., Shakouri, A., Abraham, P., Bowers, J.E., 2000, "Monolithic Integration of Thin-Film Coolers with Optoelectronic Devices," Optical Engineering, **39**, pp. 2847-2852.

[9] LaBounty, C; Shakouri, A; Bowers, JE., 2001, "Design and characterization of thin film microcoolers," J. Applied Physics, **89**, pp. 4059-4064.

[10] Whitlow, L.W. and Hirano, T., 1995, "Superlttice Application to Thermoelectricity," J. Applied Physics, **78**, pp. 5460-5466.

[11] Mahan, G.D. and Woods, L.M., 1998, "Multilayer Thermionic Refrigeration," Physical Review Letters, **80**, pp. 4016-4019 (1998).

[12] Moyzhes, B. and Nemchinsky, V**.,** 1998, "Thermoelectric Figure of Merit of Metal-Semiconductor Barrier Structure based on Energy Relaxation Length**,"** Applied Physics Letters, **73**, pp.1895-1897.

[13] C. B. Vining and G. D. Mahan, Journal of Applied Physics 86, 6852-3 (1999).

[14] Ulrich, M.D.; Barnes, P.A.; Vining, C.B. Comparison of solid-state thermionic refrigeration with thermoelectric refrigeration. Journal of Applied Physics, vol.90, (no.3) 2001. p.1625-31.

[15] Radtke, R.J., Ehrenreich, H., and Grein, C.H., 1999, "Multilayer Thermoelectric Refrigeration in $Hg_{1-x}Cd_xTe$ Superlattices," J. Applied Physics, **86**, pp. 3195-3198.

[16] Zeng, T.F. and Chen, G., 2000, "Energy Conversion in Heterostructures for Thermionic Cooling," Microscale Thermophysical Engineering, **4**, pp. 39-50.

[17] Harman, T.C., Taylor, P.J., Spears, D.L., and Walsh, M.P., 2000, "Thermoelectric Quantum-Dot Superlattices with High ZT," J. Electronic Materials, **29**, pp. L1-L4.

[18] Chen, G., 2001, "Phonon Transport in Low-Dimensional Structures" Semiconductors and Semimetals, **71**, pp. 203-259.

[19] Venkatasubramanian, R., 2001, "Phonon Blocking Electron Transmitting Superlattice Structures as Advanced Thin Film Thermoelectric Materials," Semiconductors and Semimetals, **71**, pp. 175-201.

[20] R. Venkatasubramanian, E. Siivola, T. Colpitts, and B. O'Quinn, Nature 413, 597-602 (2001).

[21] S.V.Meshkov, Sov. Phys. JETP 64 (6), December 1986

[22] B.F. Levine, C.G. Bethea, G. Hanian, V.O. Shen, E. Pelve, R.R. Abbott, and S.J. Hsieh, Appl. Phys. Lett. 56(9), 26 February 1990

[23] E. Pevle´, F. Beltram, C.G. Bethea, B'F. Levine, V.O. Shen, S.J. Hsieh, and R.R. Abboth, J. Appl. Phys, 66(11), 1 December 1989

[24] I. V. Kukushkin and V.B. Timofeev, Pis'ma Zh. Eksp. Teo. Fiz. 40, 413 (1984) [JETP Lett. 40, 1231 (1984)]

[25] V. D. Kulakoviskii, B. N. Shepel', A. A. Denisov, and A. P. Senichkin, Fiz. Tekh. Poluprovodn. 21, (1987) [sic].